Acta Crystallographica Section D
Biological Crystallography
ISSN 0907-4449

Crystallization and preliminary crystallographic data of 2-enoyl-CoA hydratase 2 domain of *Candida tropicalis* peroxisomal multifunctional enzyme type 2

M. Kristian Koski, Antti M. Haapalainen, J. Kalervo Hiltunen and Tuomo Glumoff*

Biocenter Oulu and Department of Biochemistry, University of Oulu, Box 3000, FIN-90014 University of Oulu, Finland

Correspondence e-mail: tuomo.glumoff@oulu.fi

Received 8 January 2003
Accepted 6 May 2003

In yeast, the second and the third reaction of the fatty-acid β-oxidation spiral are catalysed by peroxisomal multifunctional enzyme type 2 (Mfe2p/Fox2p). This protein has two (3*R*)-hydroxyacyl-CoA dehydrogenase domains and a C-terminal 2-enoyl-CoA hydratase 2 domain. Here, the purification, crystallization and X-ray diffraction analysis of the hydratase 2 domain [CtMfe2p($dh_{a+b}\Delta$)] from *Candida tropicalis* Mfe2p is reported. CtMfe2p($dh_{a+b}\Delta$) was overexpressed as an enzymatically active recombinant protein and crystallized by the hanging-drop vapour-diffusion method. The crystals belong to space group *C*2, with unit-cell parameters $a = 178.57$, $b = 60.46$, $c = 130.85$ Å, $\beta = 94.48^\circ$. Selenomethionine-labelled protein was used for a multi-wavelength anomalous dispersion (MAD) experiment. A three-wavelength data set suitable for MAD phasing was collected to 2.25 Å resolution using synchrotron radiation.

1. Introduction

Multifunctional enzymes (MFEs), which catalyse the second and third reaction of the β-oxidation spiral of fatty acids, are found in many organisms independent of subcellular localization (Hiltunen, 2002). Mammalian peroxisomes have two MFEs, types 1 and 2 (MFE-1 and MFE-2), which are not related by amino-acid sequence. MFE-1 has 2-enoyl-CoA hydratase 1/(3*S*)-hydroxyacyl-CoA dehydrogenase activity, while MFE-2 has 2-enoyl-CoA hydratase 2/(3*R*)-hydroxyacyl-CoA dehydrogenase activity (Lalwani *et al.*, 1981; Leenders *et al.*, 1994; Osumi & Hashimoto, 1979; Qin, Poutanen *et al.*, 1997; Uchida *et al.*, 1992). Mammalian peroxisomal MFE-1 has an additional Δ^3-Δ^2-dienoyl-CoA isomerase activity in its hydratase 1 domain (Kiema *et al.*, 2002; Palosaari & Hiltunen, 1990). In contrast to mammalian peroxisomes, yeast/fungi peroxisomes have only one MFE, Mfe2p/Fox2p (Hiltunen *et al.*, 1992; Nuttley *et al.*, 1988).

Mfe2p shares amino-acid sequence similarity with mammalian MFE-2. The hydratase 2 domain in both Mfe2p and MFE-2 is preceded by the (3*R*)-hydroxyacyl-CoA dehydrogenase domain. However, the dehydrogenase domain in the yeast protein is duplicated and both domains are enzymatically active (Qin *et al.*, 1999; Qin, Poutanen *et al.*, 2000). Furthermore, Mfe2p lacks the C-terminal SCP-2-like domain present in its mammalian homologue.

Since fungi lack the mitochondrial β-oxidation system, peroxisomal Mfe2p is solely responsible for the degradation of fatty acids to acetyl-CoA. In contrast, mammalian peroxisomal MFEs contribute to β-oxidation, metabolizing those substrates which are not or are only slowly oxidized by mitochondrial β-oxidation. Hence, substrates such as CoA esters of very long chain polyunsaturated and α-branched fatty acids, long-chain dicarboxylic acids and prostaglandins, as well as intermediates of bile-acid synthesis, are β-oxidized in mammalian peroxisomes (Dieuaide-Noubhani *et al.*, 1997; Hashimoto, 1999; Hiltunen *et al.*, 1992; Novikov *et al.*, 1997; Palosaari & Hiltunen, 1990; Qin, Haapalainen *et al.*, 1997; Reddy & Mannaerts, 1994).

This work focuses on the 2-enoyl-CoA hydratase 2 domain of *Candida tropicalis* Mfe2p [CtMfe2p($dh_{a+b}\Delta$)]. Our previous work on mammalian MFE-2 proteins has identified a conserved amino-acid sequence motif which is also present in CtMfe2p($dh_{a+b}\Delta$) (Qin, Haapalainen *et al.*, 2000). A high-resolution crystal structure of 2-enoyl-CoA hydratase 2 would give us a more detailed insight into the reaction mechanism of this essential enzyme. Here, we present preliminary crystallization studies of CtMfe2p($dh_{a+b}\Delta$).

2. Materials and methods

2.1. Overexpression and purification

The plasmid pMK/HDE50 encoding *C. tropicalis* Mfe2p was a gift from Dr R. A. Rachubinski (Aitchison *et al.*, 1991). pMK/HDE50 was used as a template for PCR amplification of a region encoding amino-acid residues 628–906 of *C. tropicalis* Mfe2p using the primers 5′-ATGCT**CATATG**GAAGACGATCCAGTCTGGAGA-3′ and 5′-ATGCT**GGATCC**TTAGATCTTTGCTTTGTCACC-

GAC-3′ (*Nde*I and *Bam*HI restriction sites are shown in bold). The PCR fragment was subcloned to a pUC-18 vector using the Sure-Clone Ligation Kit (Amersham Biosciences). The 890 bp insert was cloned from the pUC-18 vector to a pET-3a expression vector (Novagen) as a *Nde*I/*Bam*HI (MBI Fermentas) fragment, resulting in the plasmid *pET3a::CtMfe2p(dh$_{a+b}$Δ)*.

Escherichia coli BL21(DE3) pLysS cells were transformed with the plasmid *pET3a::CtMfe2p(dh$_{a+b}$Δ)*. A single colony was chosen and grown overnight at 310 K in Luria–Bertani broth containing 50 µg ml^{-1} carbenicillin and 34 µg ml^{-1} chloramphenicol. A 10 ml portion of an overnight culture was transferred to 1 l of M9ZB medium (supplemented with carbenicillin and chloramphenicol) and bacterial cells were grown under aerobic conditions until an OD_{600} of 0.6 was reached. The temperature was shifted from 310 to 303 K and expression of recombinant protein was initiated by the addition of isopropyl-β-D-thiogalactopyranoside (IPTG) to 0.4 m*M*. After 3 h of induction, cells were collected by centrifugation and washed with cold 16 m*M* potassium phosphate, 120 m*M* NaCl pH 7.4. 4 g of bacterial cell pellet was lysed by suspension in 40 ml 25 m*M* 3-(cyclohexylamino)-1-propanesulfonic acid (CAPS), 5 m*M* EDTA, 1 m*M* DDT, 0.5 m*M* benzamidine hydrochloride hydrate pH 10 (buffer *A*) containing 100 µg ml^{-1} lysozyme, 25 µg ml^{-1} DNase I, 25 µg ml^{-1} RNase A, 10 m*M* $MgCl_2$ and 0.01 m*M* phenylmethylsulfonyl fluoride (PMSF). After 15 min incubation at 294 K, the soluble fraction containing the recombinant protein was separated from the cell debris by centrifugation (30 000*g*, 45 min, 277 K).

The supernatant was applied at a flow rate of 1 ml min^{-1} to a Q-Sepharose anion-exchange column (2.5 × 10 cm; Amersham Biosciences) pre-equilibrated in buffer *A*. The purest fractions of CtMfe2p(dh$_{a+b}$Δ) were found in the flowthrough from the column when the column was heavily overloaded. The first 20 ml of flowthrough was combined and dialyzed overnight against 1 l 25 m*M* Tris–HCl, 5 m*M* EDTA pH 8.5 (buffer *B*). The dialyzed sample was applied to a Resource Q column (6 ml; Amersham Biosciences) pre-equilibrated with buffer *B*; bound CtMfe2p(dh$_{a+b}$Δ) was eluted with a linear NaCl gradient (0–0.2 *M* in 120 ml). Fractions containing CtMfe2p(dh$_{a+b}$Δ) were pooled and dialyzed overnight against 50 m*M* sodium phosphate, 5 m*M* EDTA, 1.5 *M* $(NH_4)_2SO_4$ pH 7.8 (buffer *C*). After dialysis, the sample was loaded onto a Resource Phenyl-Sepharose Fast-Flow hydrophobic interaction column (1 ml; Amersham Biosciences) equilibrated with buffer *C* and the bound protein was eluted with a linear gradient of $(NH_4)_2SO_4$ (1.5–0 *M* in 20 ml). The CtMfe2p(dh$_{a+b}$Δ)-containing fractions were pooled and dialyzed against 30 m*M* *N*-(2-hydroxyethyl)piperazine-*N*′-(2-ethanesulfonic acid) (HEPES), 30 m*M* NaCl, 1 m*M* EDTA, 1 m*M* sodium azide (NaN_3) pH 8.0 (buffer *D*). The sample was then concentrated using an Ultrafree concentrator unit with a molecular-weight cutoff of 10 kDa (Millipore) and then applied to a Superdex200 HR 10/30 column (Amersham Biosciences) equilibrated with buffer *D*. The peak fractions from the size-exclusion column were pooled and concentrated. After every purification step, the purity of the protein was monitored by Coomassie-stained SDS–PAGE. Activity measurements were based on the formation of the magnesium complex of 3-ketoacyl-CoA from *trans*-2-decenoyl-CoA, as described previously (Hiltunen *et al.*, 1989). Protein concentrations for purified samples were measured by UV-absorbance, using a theoretical extinction coefficient of 29 870 *M* cm^{-1} at 280 nm.

To generate CtMfe2p(dh$_{a+b}$Δ) labelled with selenomethionine (SeMet), the plasmid *pET3a::CtMfe2p(dh$_{a+b}$Δ)* was transformed to the methionine-auxotrophic *E. coli* strain B834(DE3). Expression of SeMet CtMfe2p(dh$_{a+b}$Δ) was performed according to the previously described procedure (Haapalainen *et al.*, 2003) and the protein was purified as per native CtMfe2p(dh$_{a+b}$Δ). All the working buffers were supplemented with DTT to a final concentration of 1 m*M*.

Table 1
Crystallization of the native and SeMet CtMfe2p(dh$_{a+b}$Δ).

	Native	SeMet
Protein solution	25 m*M* HEPES pH 8.0, 30 m*M* NaCl, 1 m*M* EDTA, 1 m*M* NaN_3	25 m*M* HEPES pH 8.0, 30 m*M* NaCl, 1 m*M* EDTA, 1 m*M* NaN_3, 1 m*M* DTT
Protein concentration (mg ml^{-1})	17.5	17.2
Precipitant solution	7.5% PEG 4000, 0.1 *M* HEPES pH 7.0	10% PEG 4000, 0.1 *M* HEPES pH 7.0
Crystallization temperature (K)	277	277
Cryosolution	23% Ethylene glycol, 12% PEG 4000, 0.1 *M* HEPES pH 7.0	20% Ethylene glycol, 14% PEG 4000, 0.1 *M* HEPES pH 7.0

2.2. Crystallization and data collection

Crystallization trials were carried out using the hanging-drop vapour-diffusion method. Initial screening for suitable crystallization conditions was performed by the sparse-matrix screening method (Jancarik & Kim, 1991; Zeelen *et al.*, 1992). Crystallization drops contained 2 µl of protein solution together with 2 µl of reservoir solution.

The crystals were soaked in cryoprotecting mother liquor and flash-frozen in a nylon CryoLoop (Hampton Research) in a cold nitrogen stream (Oxford Cryosystems) before data collection. Crystals were first tested in the home laboratory with a rotating-anode generator (Nonius) equipped with a MAR 345 image plate (X-ray Research), but the actual data sets were collected using synchrotron radiation. Native data were collected at MAX-lab, Lund, Sweden, on beamline I711 with a MAR 345 image plate (X-ray Research) and the MAD data were collected on a single SeMet crystal at the BW7A beamline, EMBL, DESY, Hamburg, Germany, with a MAR CCD 165 mm detector (X-ray Research). All data sets were refined and scaled using *DENZO* and *SCALEPACK* from the *HKL* package (Otwinowski & Minor, 1997). Initial phases were obtained by analysis of the anomalous signal produced by Se atoms. Heavy-atom positions were searched for using the program *SOLVE* (Terwilliger & Berendzen, 1999).

3. Results and discussion

3.1. Protein expression and purification

Recombinant CtMfe2p(dh$_{a+b}$Δ) and its SeMet analogue were expressed and purified to homogeneity, as determined by SDS–PAGE. Based on size-exclusion chromatography, both proteins were dimeric with an apparent molecular weight of 63 kDa. However, a small fraction (∼5%) of native CtMfe2p(dh$_{a+b}$Δ) appeared to be tetrameric at a salt concentration of 150 m*M* (as used in buffer *D*). Decreasing the salt concentration to 30 m*M* in the last purification step resulted in the presence of a single elution peak from size-exclusion chromatography with the retention time of the dimeric form. The k_{cat} value for purified native CtMfe2p(dh$_{a+b}$Δ) with *trans*-2-decenoyl-CoA was 388 s^{-1}, which is close to the value

Table 2
Refinement statistics for native and SeMet crystals of CtMfe2p($dh_{a+b}\Delta$).

Values in parentheses are for the highest resolution shell.

Data set	Native	SeMet1 (absorption peak)	SeMet2 (absorption edge)	SeMet3 (high-energy remote)	SeMet4 (high resolution)
Beamline	I711, MAX-lab, Lund	BW7A, EMBL, DESY, Hamburg	BW7A, EMBL, DESY, Hamburg	BW7A, EMBL, DESY, Hamburg	BW7A, EMBL, DESY, Hamburg
Wavelength	0.959150	0.979852	0.980322	0.961123	0.979852
Space group	*C*2	*C*2	*C*2	*C*2	*C*2
Unit-cell parameters					
a (Å)	178.57	178.81	178.80	178.81	178.78
b (Å)	60.46	60.65	60.64	60.64	60.55
c (Å)	130.85	131.11	131.10	131.10	131.05
β (°)	94.48	94.59	94.59	94.59	94.62
No. observations	279175	282927	281758	281582	173224
No. unique reflections	79062	66926	66850	66865	93849
Multiplicity	3.5	4.2	4.2	4.2	1.8
Resolution range (Å)	15–2.10 (2.14–2.10)	25–2.25 (2.33–2.25)	25–2.25 (2.33–2.25)	25–2.25 (2.33–2.25)	25–1.90 (1.97–1.90)
Completeness (%)	97.9 (86.7)	100 (100)	100 (100)	100 (100)	85.0 (88.2)
R_{merge} (%)	4.4 (17.2)	4.3 (11.8)	4.0 (16.5)	4.2 (14.5)	4.7 (30.0)
$I/\sigma(I)$	25.76 (6.50)	24.96 (12.05)	30.80 (8.90)	27.4 0 (10.00)	12.35 (2.25)

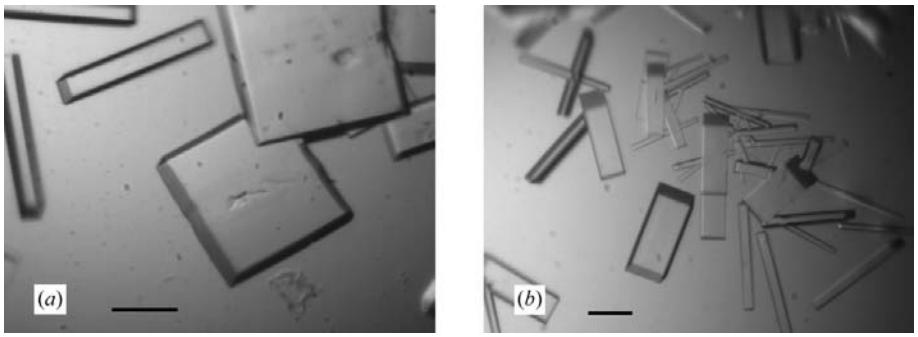

Figure 1
Crystals of (*a*) native and (*b*) SeMet CtMfe2p($dh_{a+b}\Delta$) from *C. tropicalis*. The bar represents 0.1 mm. Crystallization conditions are given in Table 1.

of 279 s^{-1} reported for the 46 kDa 2-enoyl-CoA hydratase 2 fragment of MFE-2 isolated from human liver (Jiang *et al.*, 1996). The incorporation of SeMet into the structure did not affect the hydratase 2 activity. A total of 2.2 mg of pure CtMfe2p($dh_{a+b}\Delta$) and 0.55 mg of pure SeMet analogue were obtained from 1 l of cell culture.

3.2. Preliminary crystal characterization

Crystallization screening was performed with native CtMfe2p($dh_{a+b}\Delta$) concentrated to 4.0 mg ml^{-1}. Initially, star-like twinned crystals were obtained in 25%(*w*/*v*) PEG 6000, 0.1 *M* triethanolamine–HCl (TEA) pH 7.5 at 294 K from protein solution containing 150 m*M* NaCl. When the influence of salt concentration on the oligomerization state of CtMfe2p($dh_{a+b}\Delta$) was observed, crystallization with the above-mentioned conditions was tried again with only 30 m*M* NaCl present. The effect was remarkable: the crystallization drops were full of plate-like microcrystals by the following day. Optimizing the conditions further by decreasing the precipitant concentration and the temperature and increasing the protein concentration to 17.5 mg ml^{-1} resulted in larger plate-like crystals (Fig. 1*a*). The optimized crystallization conditions are presented in Table 1. Strong precipitation was observed in the drops immediately after setting up the crystallization experiment, followed by small crystals on day one and crystals of dimensions 0.2 × 0.2 × 0.05 mm on day two. Prior to flash-freezing at 100 K, the plate-like crystals were incubated for 10 min in cryosolution (Table 1). On the home source these crystals diffracted to about 3 Å, but using synchrotron radiation the resolution could be improved to 1.9 Å. The crystals belonged to space group *C*2, with unit-cell parameters $a = 178.57$, $b = 60.46$, $c = 130.85$ Å, $\beta = 94.48°$. Assuming two dimers in the asymmetric unit, the Matthews coefficient V_M was calculated to be 2.82 $Å^3\ Da^{-1}$, indicating a solvent content of 56%. A native data set with an R_{merge} of 4.4% was collected and could be processed to 2.1 Å resolution using an oscillation range of 0.25° (Table 2).

SeMet CtMfe2p($dh_{a+b}\Delta$) concentrated to 17.2 mg ml^{-1} was crystallized under nearly the same conditions as the native protein (Table 1). Crystals appeared in the crystallization drop in 2 days. The crystals chosen for data collection were more rectangular than plate-like (Fig. 1*b*), but the space group and the unit-cell parameters were practically the same as for the native protein (Table 1). 20%(*v*/*v*) ethylene glycol, 14%(*w*/*v*) PEG 4000 and 0.1 *M* HEPES pH 7.0 was used as the cryoprotecting solution, in which the crystal was incubated for 5 min before flash-freezing. The complete MAD data from the SeMet-labelled crystal were collected to a resolution of 2.25 Å. A clear peak at 12 653.5 eV in the Se *K* edge fluorescence scan confirmed the presence of selenium in the crystal. 0.5° oscillation frames of data were first collected from the absorption peak (12 653.5 eV, $\lambda = 0.979852$ Å), followed by data sets from the inflection point (12 647.4 eV, $\lambda = 0.980322$ Å) and from the high-energy remote point (12 900.0 eV, $\lambda = 0.961123$ Å). To secure as much data as possible for the structure solution, an additional data set to 1.90 Å resolution was subsequently collected from the absorption peak. The statistics of data collection are presented in Table 2.

If the initial methionine residue is present, a total of 16 Se atoms would be expected to be present in the asymmetric unit of the SeMet CtMfe2p($dh_{a+b}\Delta$) crystal. The first eight selenium sites were found and refined using *SOLVE*. Currently, the figure of merit of the experimental phases is 0.56. Further improvement of the phases is in progress.

This work was supported by the European Community (Access to Research Infrastructure Action of the Improving Human Potential Programme to the EMBL Hamburg Outstation, Contract No. HPRI-

1999-CT-00017) and by grants from the Academy of Finland and Sigrid Jusélius Foundation. We acknowledge the staff at the EMBL, DESY, Hamburg and MAX-lab, Lund for the opportunity to collect data at the beamlines BW7A and I711, respectively. We also thank Marika Kamps, Eeva-Liisa Stefanius and Ville Ratas for technical assistance.

References

Aitchison, J. D., Sloots, J. A., Nuttley, W. M. & Rachubinski, R. A. (1991). *Gene*, **105**, 135–136.

Dieuaide-Noubhani, M., Novikov, D., Vandekerckhove, J., Veldhoven, P. P. & Mannaerts, G. P. (1997). *Biochem. J.* **321**, 253–259.

Haapalainen, A. M., Koski, M. K., Qin, Y.-M., Hiltunen, J. K. & Glumoff, T. (2003). *Structure*, **11**, 87–97.

Hashimoto, T. (1999). *Neurochem. Res.* **24**, 551–563.

Hiltunen, J. K. (2002). *Wiley Encyclopedia of Molecular Medicine*, edited by H. H. Kazazian, Vol. 5, pp. 3240–3243. New York: John Wiley & Sons.

Hiltunen, J. K., Palosaari, P. M. & Kunau, W. H. (1989). *J. Biol. Chem.* **264**, 13536–13540.

Hiltunen, J. K., Wenzel, B., Beyer, A., Erdmann, R., Foss, A. & Kunau, W. H. (1992). *J. Biol. Chem.* **267**, 6646–6653.

Jancarik, J. & Kim, S.-H. (1991). *J. Appl. Cryst.* **24**, 409–411.

Jiang, L. L., Kobayashi, A., Matsuura, H., Fukushima, H. & Hashimoto, T. (1996). *J. Biochem.* **120**, 624–632.

Kiema, T. R., Taskinen, J. P., Pirilä, P. L., Koivuranta, K. T., Wierenga, R. K. & Hiltunen, J. K. (2002). *Biochem. J.* **367**, 433–441.

Lalwani, N. D., Reddy, M. K., Mangkornkanok-Mark, M. & Reddy, J. K. (1981). *Biochem. J.* **198**, 177–186.

Leenders, F., Husen, B., Thole, H. H. & Adamski, J. (1994). *Mol. Cell. Endocrinol.* **104**, 127–131.

Novikov, D., Dieuaide-Noubhani, M., Vermeesch, J. R., Fournier, B., Mannaerts, G. P. & Van Veldhoven, P. P. (1997). *Biochim. Biophys. Acta*, **1360**, 229–240.

Nuttley, W. M., Aitchison, J. D. & Rachubinski, R. A. (1988). *Gene*, **69**, 171–180.

Osumi, T. & Hashimoto, T. (1979). *Biochem. Biophys. Res. Commun.* **89**, 580–584.

Otwinowski, Z. & Minor, W. (1997). *Methods Enzymol.* **276**, 307–326.

Palosaari, P. M. & Hiltunen, J. K. (1990). *J. Biol. Chem.* **265**, 2446–2449.

Qin, Y.-M., Haapalainen, A. M., Conry, D., Cuebas, D. A., Hiltunen, J. K. & Novikov, D. K. (1997). *Biochem. J.* **328**, 377–382.

Qin, Y.-M., Haapalainen, A. M., Kilpelainen, S. H., Marttila, M. S., Koski, M. K., Glumoff, T., Novikov, D. K. & Hiltunen, J. K. (2000). *J. Biol. Chem.* **275**, 4965–4972.

Qin, Y.-M., Marttila, M. S., Haapalainen, A. M., Siivari, K. M., Glumoff, T. & Hiltunen, J. K. (1999). *J. Biol. Chem.* **274**, 28619–28625.

Qin, Y.-M., Poutanen, M. H., Helander, H. M., Kvist, A. P., Siivari, K. M., Schmitz, W., Conzelmann, E., Hellman, U. & Hiltunen, J. K. (1997). *Biochem. J.* **321**, 21–28.

Qin, Y.-M., Poutanen, M. H. & Novikov, D. K. (2000). *J. Lipid. Res.* **41**, 93–98.

Reddy, J. K. & Mannaerts, G. P. (1994). *Annu. Rev. Nutr.* **14**, 347–370.

Terwilliger, T. C. & Berendzen, J. (1999). *Acta Cryst.* D**55**, 849–861.

Uchida, Y., Izai, K., Orii, T. & Hashimoto, T. (1992). *J. Biol. Chem.* **267**, 1034–1041.

Zeelen, J. P., Pauptit, R. A., Wierenga, R. K., Kunau, W. H. & Hiltunen, J. K. (1992). *J. Mol. Biol.* **224**, 273–275.